The 11th Canadian Conference on Earthquake Engineering
Canadian Association for Earthquake Engineering

EFFECT OF ROTATION ON THE HORIZONTAL BEHAVIOR OF RUBBER ISOLATORS

Saman RASTGOO MOGHADAM
PhD Candidate, McMaster University, Canada
rastgos@mcmaster.ca

Dimitrios KONSTANTINIDIS
Assistant Professor, McMaster University, Canada
konstant@mcmaster.ca

ABSTRACT: Seismic isolation is an earthquake-resistant design approach where a horizontally flexible layer is introduced in a structure to decouple the superstructure from the motion of the substructure. In buildings, traditional practice places the isolation layer at the foundation level and calls for the construction of rigid diaphragms above and below the isolation layer. During an earthquake, these rigid diaphragms cause the isolators to displace horizontally and vertically but experience no rotation. More recently, however, structural designers have been exploring creative ways to reduce or eliminate these costly rigid diaphragms. In these innovative designs, aside from vertical and relative lateral displacements, the isolators also experience rotations. Past experimental and analytical studies have investigated the horizontal behavior of rubber isolators under the assumption of zero top and bottom rotation. These studies have characterized the effect of vertical load on the lateral stiffness of a rubber bearings and the lateral stability limit (defined as the displacement at which the tangent stiffness becomes zero). This paper investigates the effect of rotation on the horizontal behavior of rubber isolators using 3D Finite Element Analysis (FEA). Three boundary conditions are considered: (1) rotation at the bottom and top of a bearing, (2) rotation only at the bottom, and (3) rotation only at the top of a bearing. The study concludes that rotation can have a significant effect on the stability of rubber isolators.

1. Introduction

Unlike conventional approaches to earthquake-resistant design, which aim at increasing the seismic capacity of a structure, seismic isolation aims at decreasing the seismic demand (Naeim and Kelly, 1999). This is achieved through the introduction of a horizontally flexible layer that in effect decouples the superstructure from the horizontal seismic excitation. The fundamental natural period of the system is shifted to the long period range, thereby decreasing the seismic demand on the superstructure and its contents (Kelly, 1986). The concept of seismic isolation became a practical reality with the development of multilayer elastomeric isolators (Naeim and Kelly, 1999), which are currently the most widely used type of isolator. These isolators are made of layers of natural or synthetic rubber interleaved with thin steel reinforcing plates (shims). A typical elastomeric isolator features thick steel end plates, bonded to the elastomer during the vulcanization process. The end plates are connected to the superstructure and substructure with bolts. More recently, the concept of unbonded isolators has received a lot of attention (Kelly, 1999; Kelly and Konstantinidis, 2007; Mordini and Strauss, 2008; Toopchi-Nezhad et al., 2011; Russo et al., 2013; Osgooei et al., 2014(b); Van Engelen et al., 2014(b), Calabrese et al., 2014). In these types of isolators, the shear force is transferred through friction that develops along the contact interface (Konstantinidis et al., 2008; Kelly and Konstantinidis, 2009; Russo and Pauletta, 2013).

Past studies have shown that elastomeric isolators under combined axial and horizontal loading behave nonlinearly (e.g., Kelly and Konstantinidis, 2011), and an individual isolator undergoing large lateral displacements may experience a decrease in its axial-load capacity. Nearly all previous experimental and

analytical studies have investigated the horizontal behavior of isolators under the assumption of zero top and bottom rotation. In reality, however, it is possible for an isolator to experience rotation. Ohsaki et al. (2015), who investigated the dynamic response of a base-isolated 10-story RC frame building using 3D FEA, noted that the elastomeric isolators experienced rotation at their supports. In applications such as isolation of high-rise buildings or mid-height isolation, the effect of rotation may be significant. The effect of rotation may also be important in bridge applications, where the seismic isolators are placed between the bridge deck and the piers or abutments can experience rotation due to flexure of the deck above the isolator or the piers below.

The determination of the lateral stability limit of elastomeric isolators is based on an extension of Euler buckling load theory proposed by Haringx (1948). This linear theory assumed a bearing is a homogenous and isotropic column that behaves as a rubber rod. Gent (1964) investigated the decrease in the horizontal stiffness of rubber bearings with increasing axial load. Stanton et al. (1990) extended the theory to account for the effect of axial shortening and provided experimentally verification. Experimental tests on the stability of modern seismic isolation elastomeric bearings under quasi-static loading have been conducted by Buckle and Kelly (1986). Buckle and Liu (1993) conducted an experimental study to determine the critical buckling load of elastomeric bearings and proposed a formula based on the so-called *Overlapping Area Method* to estimate the critical load, which is used in practice nowadays, although further experimental study showed that this formula is overly conservative, especially at lateral displacements equal to the bearing diameter or width (Buckle, et al., 2002, Cardone and Perrone, 2012). Recently Sanchez et al. (2012) carried out a comprehensive experimental program to examine the stability of bearings under quasi-static and dynamic loading. The advantage of dynamic testing is realistic simulation of seismic loadings conditions and quantification of the response of elastomeric bearings at beyond their stability limit.

Beside experimental investigations, there have been several analytical and numerical studies investigating the stability of elastomeric bearings. Koh and Kelly (1988) proposed a simple mechanical model including both shear and flexural deformations, to study the stability of elastomeric isolations. They compared the results of this model with experimental results for natural rubber bearings; it was shown that the model captured the behavior with good accuracy. Koo et al (1999) modified the Koh-Kelly model by using an instantaneous apparent shear modulus obtained from test results instead of a constant shear modulus value. In Koo et al (1999), the shear modulus is a function of the shear strain and can be presented by a polynomial equation obtained by least squares fitting of test results. The advantage of this modification is elimination of imprecision associated with in the constant shear modulus. Nagarajaiah and Ferrell (1999) extended the Koh-Kelly model to include large displacements. They showed that the critical load and horizontal stiffness decreases with increasing lateral displacement. Iizuka (2000) developed a model by introducing finite deformation and nonlinear springs into the Koh-Kelly model. From experimental and analytical results, this model accurately captures the characteristics of elastomeric bearings, such as hardening, load deterioration, and buckling phenomena. The nonlinear parameters of the rotational and shear springs in the model are determined through experimental testing. The advantage of this model is that it can easily handle a variable axial force. A three-dimensional model which includes multiple shear springs at the mid-height and a series of axial springs at the top and bottom of an isolator was proposed by Yamamoto et al. (2009) and Kikuchi et al. (2010) for circular and rectangular isolatros, respectively. Han and Warn (2014) conducted sensitivity analysis on previous models using FEA and proposed an alternative model which does not rely on experimentally calibrated parameters. This model includes a series of vertical springs with simple bilinear constitutive relationship. These vertical springs replace the rotational spring which was used in the Koh-Kelly model. The solution process to find the critical point is similar in the Izuka model. Vemuru et al. (2014) showed that the Nagarajaiah-Ferrell model cannot accurately predict the stiffness degradation beyond the stability point. As this model is based on quasi-static tests, the stiffness of the bearings beyond the stability limit is larger than that expected by the model. Vemuru et al. (2014) modified the Nagarajaiah-Ferrell model by incorporating higher order displacement terms in the rotational spring. The model is capable of characterizing the dynamic behavior of bearings more accurately than previous models, particularly beyond the instability point. Kumar et al. (2014) proposed a new model to account for cyclic vertical and horizontal loadings. This model can describe the behavior of elastomeric isolation bearings in tension, including the cavitation and post-cavitation bahvior.

The use of FEA is a common approach to understand the behavior of rubber isolators. Recently, studies using this approach have evaluated the behavior of isolation bearings under compression and shear, as well as their stability. Mordini and Strauss (2008) presented an isolation system consisting of high damping rubber bearings reinforced with glass fiber fabric. This parametric study using FEA examined the vertical and horizontal behavior of bearings with Neo-Hookean and Ogden rubber material models. Nguyen and Tassoulas (2009) used ABAQUS to model a square and a rectangular unbonded steel-reinforced elastomeric bearing in 3D under compressive load accompanied by shear in various lateral directions including longitudinal and transverse directions. A constitutive model based on the Yeoh strain energy density function was used to represent the behavior of the rubber. Their results showed that there was no significant effect of the shear direction on the stiffness at 50 percent shear displacement. Toopchi-Nezhad et al. (2011) compared the behaviour of Fiber Reinforced Elastomeric Isolators (FREI) in unbonded and bonded applications. Osgooei et al. (2014(a)) used 3D FEA to study the behavior of circular fiber-reinforced elastomeric bearings under compression. Osgooei et al. (2014(b)) investigated the lateral response of unbonded FREIs when loaded in deferent directions. The behavior of unbonded FREIs that feature geometric modifications was investigated under pure compression (Van Engelen et al., 2014(a)) and compression and shear (Osgooei et al., 2015). Warn and Weisman (2011) conducted a parametric study to investigate the effect of geometry on the critical load of rubber bearings using 2D FEA. Their results showed that the critical load is more sensitive to the bearing width and the individual rubber layer thickness than it is to the number of rubber layers. Weisman and Warn (2012) used experimental testing and FEA to investigate the critical load capacities of an elastomeric bearing and a lead-rubber bearing with shape factor values of 10 and 12, respectively. The results of this investigation showed that the lead core does not have a significant effect on the critical load over a range 150-280 percent shear strain in comparison with elastomeric bearings without a lead core.

The main objective of this study is to investigate the effect of rotation on the horizontal behavior of isolation bearings. A 3D finite element model of a circular elastomeric bearing is developed in ABAQUS (2010) and evaluated by comparing FEA results with the analytical solution presented by Karbakhsh Ravari et al. (2012), which is applicable for studying the horizontal behavior of rubber bearings before the instability point. Subsequently, the effects of rotation and pressure on the critical load of an elastomeric bearing are studied.

2. Verification of the Finite Element Analysis

The original theory for the buckling of elastomeric isolations is based on Haringx's studies on the stability of solid rubber rods (Haringx, 1948). Later, this theory was applied by Gent (1964) to solve the problem of the stability of multilayer rubber compression springs. Other researchers proposed a linear method to account for the behavior of isolation bearings under vertical and lateral forces (Kelly and Konstantinidis, 2011). This approach suggests that an individual bearing can be modeled as a homogeneous and isotropic column and the column height is the total thickness of the rubber layers and steel shims. The method can be used to study P-Δ effects. Chang (2002) and Karbakhsh Ravari et al. (2012) applied this theory to the case where the supports experienced rotation to study its effect on the behavior of the elastomeric bearings under vertical and lateral forces. This approach is used to verify the finite element model used in this study. The details of the theoretical analysis are presented in Karbakhsh Ravari et al. (2012). Based on this procedure, the maximum horizontal displacement, u_{max}, on the top of the bearing due to the horizontal force, H, the axial load, P (which are applied on the top of the bearing) and the rotation at the top, θ_T, and/or at the bottom, θ_B, of the bearing is obtained by,

$$u_{max} = c_1\left(\cos(\alpha h)-1\right)+c_2\sin(\alpha h)-\frac{P\theta_B-H}{P+H\theta_B}h \tag{1}$$

where h is the total height of the bearing including the rubber layers and steel shims. c_1 and c_2 are obtained by,

$$c_1 = c_2\cot(\alpha h)-\frac{\csc(\alpha h)}{\alpha\beta}\left[\theta_T-\frac{P\theta_B-H}{P+H\theta_B}+\frac{(P\theta_B-H)H\theta_B}{(P+H\theta_B)(GA_s+P)}\right] \tag{2}$$

$$c_2 = \frac{1}{\alpha\beta}\left[\theta_B - \frac{P\theta_B - H}{P + H\theta_B} + \frac{\left(P\theta_B - H\right)H\theta_B}{\left(P + H\theta_B\right)\left(GA_s + P\right)}\right] \tag{3}$$

where α and β are defined by

$$\alpha = \sqrt{\frac{\left(GA_s + P\right)\left(P + H\theta_B\right)}{EI_s}} \quad ; \quad \beta = \frac{GA_s}{GA_s + P} \tag{4}$$

where E and G are the Young's and shear modulus of the elastomer, respectively; $A_s = Ah/t_r$, where t_r is the total thickness of the rubber layers and A is the cross-sectional area; EI_s is the bending stiffness of the composite system, which for a circular bearing with incompressible rubber is $EI_s = (h/t_r)G\pi R^6/(8t^2)$, where R is the radius of the steel shim and t is the thickness of an individual rubber layer.

In order to compare the results of FEA with the analytical solution, the circular elastomeric bearing similar to Karbakhsh Ravari et al. (2012) shown in Fig. 1(a) was modeled. The radius of the bearing is R = 140 mm. There are 20 individual rubber layers (n_r = 20). The thickness of each layer is t = 10 mm, providing a total thickness of rubber t_r = 200 mm. The thickness of steel shims is t_s = 2 mm and each top and bottom end plate is 21 mm thick with a radius of 160 mm.

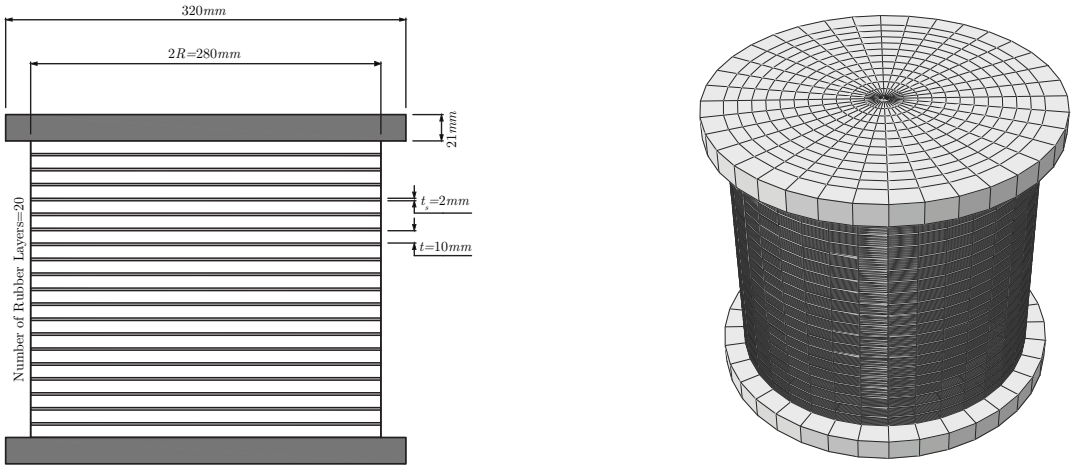

(a) (b)

Fig. 1 – (a) Cross section and (b) Finite Element mesh of the circular laminated rubber bearing

Figure 1(b) shows the mesh of the model. The rubber material is discretized with a combination of 8-node linear brick, hybrid, constant pressure (C3D8H) elements and 6-node linear triangular prism, hybrid, constant-pressure (C3D6H) elements ABAQUS (2010). Each integration point's volume of incompressible material should remain constant during the deformation, which can cause volumetric locking. To prevent this issue, ABAQUS provides a hybrid formulation in which the pressure and displacement fields are treated independently. In fact, hybrid elements include more variables to assuage the volumetric locking problem (ABAQUS, 2010). The steel material including the shims and end-plates are discretized with 8-node linear brick, incompatible modes (C3D8I) elements. Shear locking is the other major numerical problem which may cause spurious shear stresses. This issue can be solved by using incompatible modes provided by ABAQUS (2010).

As the rubber layers experience large deformations and displacements during the analysis, a hyperelastic material model is used for the rubber. The stresses in such a model are derived from a stored strain energy density function. For the compressible Neo-Hookean model used in this study the strain energy function is (Bathe, 1995)

$$W = C_{10}\left(\bar{I}_1 - 3\right) + \frac{1}{D_1}\left(J - 1\right)^2 \tag{5}$$

where C_{10} = G/2, D_1 = 2/K (where K is the bulk modulus) are model constants, $\overline{I}_1$ is the first reduced invariant (deviatoric part only) of the left Cauchy-Green deformation tensor, and J is the elastic volume ratio. In the model developed for this study C_{10} = 0.31 MPa (corresponding to G = 0.611 MPa) and the D_1 = 2×10^{-6} mm^2/N, assuming incompressible rubber. The steel shims and end plates are modeled with linear elastic material with E = 200 GPa and a Poisson's ratio ν = 0.3.

In the model, all nodes at the top end plate are constrained to a point located at the centroid of the end plate. The displacement and force (horizontal and axial load) boundary conditions are assigned to this point. The control node is free to move vertically and laterally in one direction and in the case of rotation, this node can rotate in the specified direction. Similar to the top end plate, all nodes at the bottom end plate are constrained to a control node. This point is restrained in all degrees of freedom except for rotation. The analysis is performed in two stages: in the first stage, the axial load and rotation value are applied to the top control node simultaneously; in the second stage, the horizontal force is applied to the top control node. The axial and horizontal load follow the nodal rotation (at the control node), i.e. the horizontal load is parallel to the top rotated surface of the bearing and axial load is perpendicular to the surface. The analysis includes nonlinear geometry, large displacements, and large strains. As such, the incremental nonlinear analysis is conducted using an updated Lagrangian formulation and Newton-Raphson iteration method.

Four boundary condition cases were considered to compare the FEA with the analytical solution:

1) No rotation of the end plates
2) Rotation at the top end plate only (control node at the top end plate)
3) Rotation at the top and bottom end plates (control node at the top and bottom end plates), and;
4) Rotation at the bottom end plate only (control node at the bottom end plate).

The rotation value in this analysis is 0.02 rad (1.15°) and the horizontal force, H, is 5 kN. A series of analyses with different values of average vertical stress is performed.

Figure 2(a) shows the deformed shape of the bearing at the end of the first stage of loading, at which the axial force is 200 kN and the rotation value is 0.02 rad at the top of the bearing, while Fig. 2(b) shows the bearing at the end of the second stage of loading, at which the horizontal force is 5 kN. Figure 3 shows a comparison between the FEA and analytical solution results for the four aforementioned cases. The figure shows that there is a good agreement between the results for all cases, thus providing confidence that the finite element model developed in ABAQUS can be used to study the effect of rotation. The figure also shows that when the bearing is under a constant average vertical stress ($\overline{p} = P / A$ in the range of 0 to 5 MPa) for the different rotation cases, the value of shear strain (u_{max} / t_r) is different. The case of rotation at the top of the bearing causes the largest u_{max} / t_r value.

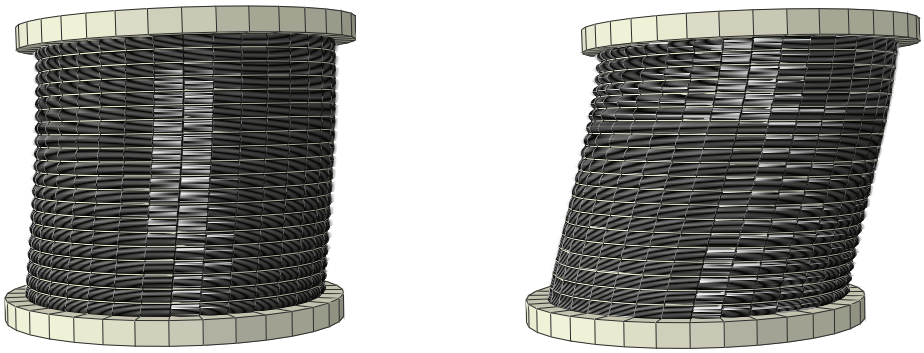

(a) (b)

Fig. 2 – Deformed shape of the bearing (P = 200 kN, H = 5 kN, $\theta_T = 0.02$ rad, and $\theta_B = 0$ rad) at (a) First stage (b) Second stage of the analysis

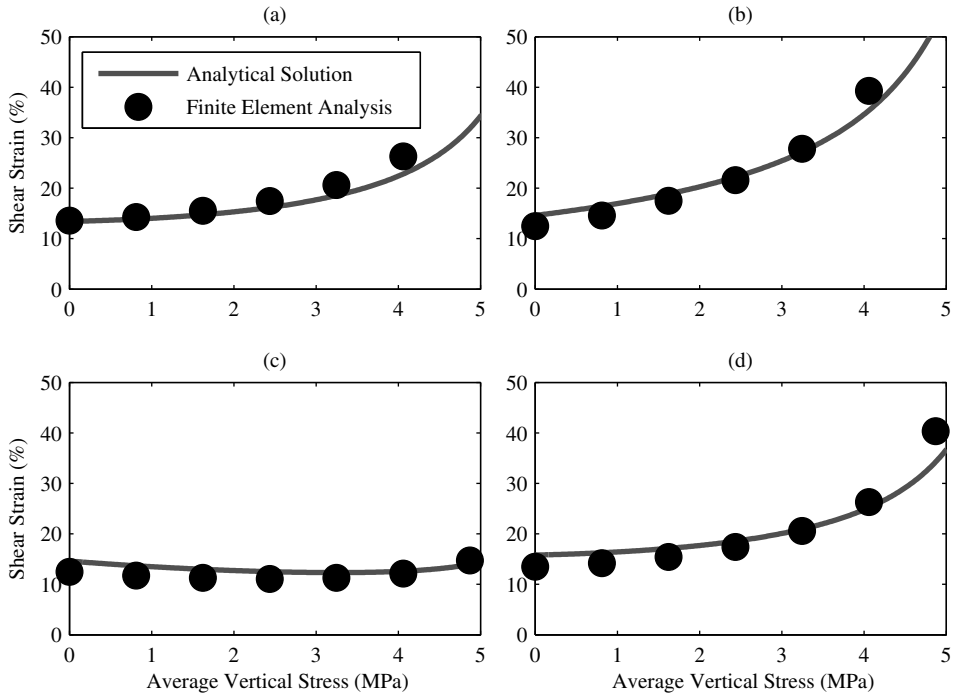

Fig. 3 – Comparison between FEA and analytical solution results (H = 5 kN) for (a) No rotation at the top or bottom of the bearing (b) Rotation at the top of the bearing only (θ_T = 0.02 rad), (c) Rotation at the bottom of the bearing only (θ_B = 0.02 rad), and (d) Rotation at the top and bottom of the bearing ($\theta_T = \theta_B$ = 0.02 rad)

3. Effect of rotation on the instability (critical) point

The *critical point* is defined as the point where the shear force attains a maximum value in the shear force-lateral displacement curve, and the tangent lateral stiffness beyond this point becomes negative. This point represents three quantities which are important in the design process: axial load, P, lateral displacement, u, and shear force, F. To obtain this point by FEA, the constant axial force method was used (Warn and Weisman, 2011). Sanchez et al. (2012) conducted experimental tests based on this method and showed that it is reliable for capturing the critical point. In this method, the u and F associated with the critical point are determined from the shear force-lateral displacement curve for a given constant P. In the loading part, the axial load is applied first, and then the horizontal displacement is applied incrementally until the horizontal stiffness becomes zero and the shear force attains its maximum value.

The loading history for the FEA in this study follows the same approach. During the first stage, the axial load but also rotation are imposed gradually until the desired values are reached. In the second stage of the analysis, the horizontal displacement is gradually increased while maintaining the axial load and rotation value from the first stage constant. Unlike the model which was described in the previous section for validation purposes, the axial load and horizontal displacement do not follow the nodal rotation. To study the effect of rotation, a circular bearing similar to Weisman and Warn (2012) with a radius R = 76 mm was modeled in 3D. The bearing had 20 rubber layers, with each layer being 3 mm thick, providing a total thickness of rubber equal to 60 mm. The bearing included 21 steel shims, each 3 mm thick. The steel material was modeled using a bilinear isotropic material model with Young's modulus of 200 GPa and a Poisson's ratio of 0.3. A post-yield modulus of 2 percent of the initial modulus was specified.

As mentioned earlier, the rubber material is described by a hyperelastic material. The main challenge is selecting a suitable hyperelastic material model, which can characterize the behavior of the rubber correctly. The Neo-Hookean material is the simplest model and assumes that the shear modulus is

constant during the analysis. Past experimental studies, however, have shown that the shear modulus is not constant, particularly at large shear strain values (Forni et al., 1999). Other hyperelastic models, using more parameters, provide better results, but they require experimental data, such as from uni-axial tension and/or shear tests, to determine the parameters. In this section, the rubber is characterized by a Mooney-Rivlin model using two parameters in addition to the bulk modulus. The strain energy potential for the Mooney-Rivlin constitutive model is

$$W = C_{10}\left(\bar{I}_1 - 3\right) + C_{20}\left(\bar{I}_2 - 3\right) + \frac{1}{D_1}\left(J-1\right)^2 \tag{6}$$

where $\bar{I}_2$ is the second reduced invariant of the left Cauchy-Green deformation tensor. It should be noted that the Neo-Hookean model can be obtained by setting C_{20} equal to zero in Eq. 6, thus obtaining the strain energy function described by Eq. 5. Material standard tests are needed to determine the constants parameters (C_{10} and C_{20}). For the purposes of this study, uni-axial tension and pure shear test results from Forni et al. (1999) are used. Figure 4 shows the results of material test for uni-axial tension and pure shear (Forni et al., 1999). The constants are obtained using curve fitting procedures in the 'material evaluation' tool available in ABAQUS (2010). C_{10} and C_{20} are 0.3904 and 0.06 MPa, respectively, and a value of 2000 MPa is assumed for the bulk modulus, *K*.

Figure 5 shows the normalized shear force-displacement curve (from the second stage of loading) for different values of rotation at the top of the bearing under a constant axial load (corresponding to $\bar{p} = 8.26$ MPa). It should be noted that the convention for positive rotation at the top is *counter-clockwise*. The figure shows that simultaneous application of the rotation and the vertical load in the first stage of loading causes lateral displacement, i.e. the lateral displacement corresponding to *F*/*GA* = 0 is different depending on the amount of rotation. This displacement value herein referred as 'Initial Displacement' increases with the rotation value and depending on the sign of the rotation value it can be positive or negative. The results show that the rotation does not affect the lateral displacement at the critical point but can change the critical shear force. For instance, rotation of 0.04 rad increases the critical shear force by 13 percent, while rotation of -0.04 rad decreases it by approximately 15 percent. Figure 6 shows the effect of rotation on the horizontal behavior of the bearing under different values of average vertical stress ($\bar{p} =$ 5.5, 8.26 and 11.02 MPa). Rotation is applied on the top of the bearing, and it varies from zero to 0.04 rad. The figure shows that increasing the pressure can increase the initial displacement (with the same rotation value). As expected, the critical shear force decreases with increasing $\bar{p}$. It is noted that for larger $\bar{p}$, the relative effect of rotation is more pronounced ,

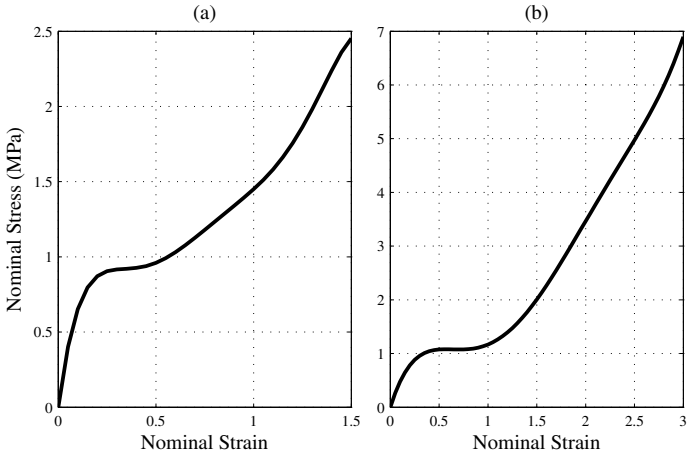

Fig. 4 – Material test results (a) Uni-axial tension (b) Pure shear (Forni et al., 1999)

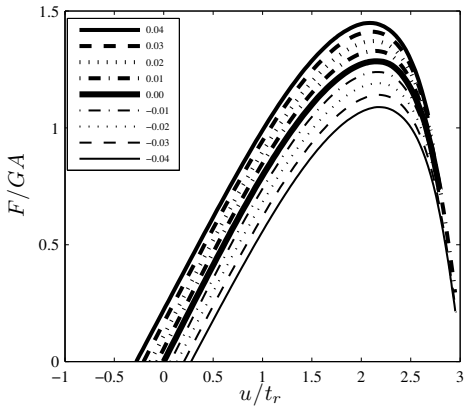

Fig. 5 – Normalized shear force-lateral displacement for different values of the rotation at the top of the bearing (-0.04 to 0.04 rad, $\bar{p}$ = 8.26 MPa)

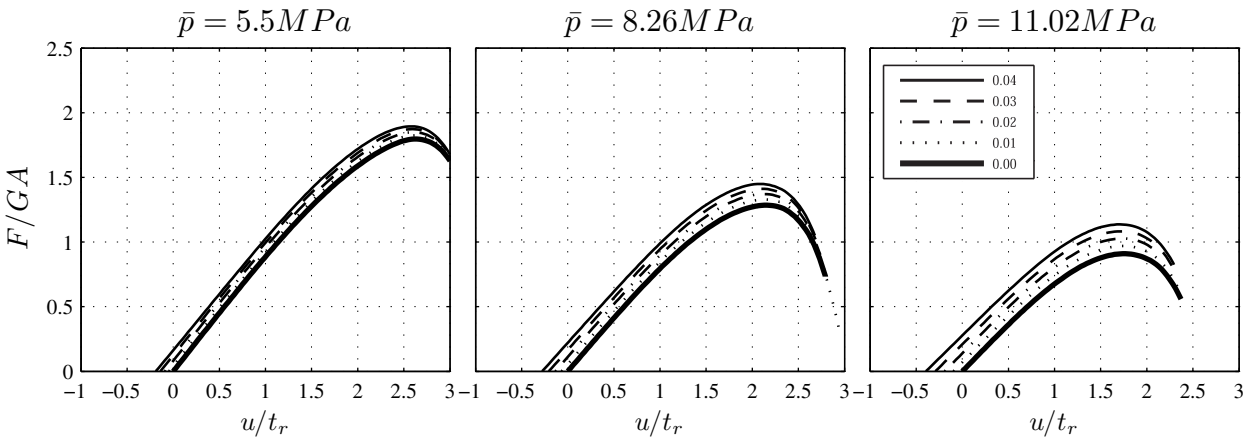

Fig. 6 – Effect of rotation on the lateral behavior of the bearing under different average vertical stress values (Rotation is applied on the top of the bearing, θ_T = 0 to 0.4 rad)

4. Conclusions

In this paper, 3D FEA of a laminated rubber bearing was carried out to validate the finite element model against an analytical solution. Four boundary conditions were considered: (1) no rotation at the top and bottom of the bearing, (2) rotation only at the top, (3) rotation only at the bottom, and (4) rotation at both the top and bottom of the bearing. It was demonstrated that the finite element model can reliably capture the effect of rotation on the horizontal behavior of the bearing. Then the effect of rotation applied to the top of another bearing was investigated under different values of average vertical stress. It was shown that applying rotation and axial load causes an initial lateral displacement that can change the lateral behavior of the bearing. The average vertical stress influences the initial lateral displacement, i.e. an increase in the average vertical stress for a given rotation value causes a larger value of initial lateral displacement. Generally, rotation does not significantly affect the critical displacement at the instability point but can decrease or increase the critical shear force. It is concluded that imposing rotation at the supports, depending on the rotation value and the average vertical stress, can appreciably influence the lateral behavior of a rubber bearing, and consequently it cannot be neglected.

5. References

ABAQUS/CAE, Version 6.10-1. Providence, USA, Dassault Systmes Simulia Cor*,* 2010.

BATHE, K.-J., *Finite Element Procedures*, New York, USA, Prentice Hall, 1995.

BUCKLE, I.G., KELLY, J.M., ‘‘Properties of Slender Elastomeric Isolation Bearings During Shake Table Studies of a Large-Scale Model Bridge Deck’’, *ACI Special Publication*, Vol. 94, 1986.

BUCKLE, I.G., LIU, H., ‘‘Stability of Elastomeric Seismic Isolation Systems’’, *Applied Technology Council (ATC)*, Redwood City, USA, 1993, pp. 293-305.

BUCKLE, I.G., NAGARAJAIAH, S., FERRELL, K., ‘‘Stability of Elastomeric Isolation Bearings: Experimental’’ *Journal of Structural Engineering*, Vol. 128, No. 1, 2002, pp. 3-11.

CALABRESE, A., SPIZZUOCO, M., SERINO, G., DELLA CORTE, G., MADDALONI, G. “Shaking Table Investigation of a Novel, Low-Cost, Base Isolation Technology Using Recycled Rubber”, *Structural Control and Health Monitoring*, Vol. 22, No. 1, 2015, pp. 107–122.

CARDONE, D., PERRONE, G., ‘‘Critical Load of Slender Elastomeric Seismic Isolators: an Experimental Perspective’’, *Engineering Structures*, Vol. 40, 2012, pp. 198-204.

CHANG, C-H., ‘‘Modeling of Laminated Rubber Bearings Using an Analytical Stiffness Matrix’’, *International Journal of Solids and Structures*, Vol. 39, No. 24, 2002, pp. 6055-6078.

FORNI, M., MARTELLI, A., DUSI, A., ‘‘Implementation and Validation of Hyperelastic Finite Element Models of High Damping Rubber Bearings’’, *Proceedings First European Conference on Constitutive Models for Rubber*, Vienna, Austria,1999, pp. 237-247.

GENT, A.N., ‘‘Elastic Stability of Rubber Compression Springs’’, *Journal of Mechanical Engineering Science*, Vol. 6, No. 4, 1964, pp. 318-326.

HAN, X., WARN, G.P., ‘‘Mechanistic Model for Simulating Critical Behavior in Elastomeric Bearings’’, *Journal of Structural Engineering*, Vol. 139, No. 12, 2014.

HARINGX, J.A., ‘‘On Highly Compressible Helical Springs and Rubber Rods and Their Application for Vibration-Free Mountings’’, *Philips Research Reports*, Vol. 13, No. 6, 1948, pp. 401-449.

IIZUKA, M., ‘‘A Macroscopic Model for Predicting Large-Deformation Behaviors of Laminated Rubber Bearings’’, *Engineering structures*, Vol. 22, No. 4, 2000, pp. 323-334.

KARBAKHSH RAVARI, A., BIN OTHMAN, I., BINTI IBRAHIM, Z., AB-MALEK, K., ‘‘P- Δ and End Rotation Effects on the Influence of Mechanical Properties of Elastomeric Isolation Bearings’’, *Journal of Structural Engineering*, Vol. 138, No. 6, 2012, pp. 669-675.

KELLY, J.M., ‘‘Aseismic Base Isolation: Review and Bibliography’’, *Soil Dynamics and Earthquake Engineering*, Vol. 5, No. 4, 1986, pp. 202-216.

KELLY, J.M., “Analysis of Fiber-Reinforced Elastomeric Isolators”, *Journal of Seismology and Earthquake Engineering*, Vol. 2, No. 1, 1999, pp. 19-34.

KELLY, J.M., KONSTANTINIDIS, D., “Low-cost Seismic Isolators for Housing in Highly-Seismic Developing Countries”, Proceedings *ASSISi 10th World Conference on Seismic Isolation, Energy Dissipation and Active Vibrations Control of Structures*, Istanbul, Turkey, 2007.

KELLY, J.M, KONSTANTINIDIS, D., “Effect of Friction on Unbonded Elastomeric Bearings”, *Journal of Engineering Mechanics*, Vol. 135, No. 9, 2009, pp. 953–960.

KELLY, J.M., KONSTANTINIDIS, D., *Mechanics of Rubber Bearings for Seismic and Vibration Isolation*, Chichester, England, Wiley, 2011.

KIKUCHI, M., NAKAMURA, T., AIKEN, I.D., ‘‘Three-dimensional Analysis for Square Seismic Isolation Bearings Under Large Shear Deformations and High Axial Loads’’, *Earthquake Engineering and Structural Dynamics*, Vol. 39, No. 13, 2010, pp. 1513-1531.

KOH, C.G., KELLY, J.M., ‘‘A Simple Mechanical Model for Elastomeric Bearings Used in Base Isolation’’, *International journal of mechanical sciences*, Vol. 30, No. 12, 1988, pp. 933-943.

KONSTANTINIDIS, D., KELLY, J.M., MAKRIS, N., *Experimental Investigation on the Seismic Response of Bridge Bearings,* EERC Report No. 2008-02, Earthquake Engineering Research Center, University of California, Berkeley, 2008.

KOO, G-H., LEE, J-H., YOO, B., OHTORI, Y., ‘‘Evaluation of Laminated Rubber Bearings for Seismic Isolation Using Modified Macro-Model with Parameter Equations of Instantaneous Apparent Shear Modulus’’, *Engineering structures*, Vol. 21, No. 7, 1999, pp. 594-602.

KUMAR, M., WHITTAKER, A.S., CONSTANTINOU, M.C., ‘‘An Advanced Numerical Model of Elastomeric Seismic Isolation Bearings’’, *Earthquake Engineering and Structural Dynamics*, Vol. 43, No. 13, 2014, pp. 1955-1974.

MORDINI, A., STRAUSS, A., ‘‘An Innovative Earthquake Isolation System Using Fibre Reinforced Rubber Bearings’’, *Engineering structures*, Vol. 30, No. 10, 2008, pp. 2739-2751.

NAEIM, F., KELLY, J.M, *Design of Seismic Isolated Structures: From Theory to Practice*, New York, USA, John Wiley & Sons, 1999.

NAGARAJAIAH, S., FERRELL, K., ‘‘Stability of Elastomeric Seismic Isolation Bearings’’, *Journal of Structural Engineering*, Vol. 125, No. 9, 1999, pp. 946-954.

NGUYEN, H., TASSOULAS, J.L., ‘‘Directional Effects of Shear Combined with Compression on Bridge Elastomeric Bearings’’, *Journal of Bridge Engineering*, Vol. 15, No. 1, 2009, pp. 73-80.

OHSAKI, M., MIYAMURA, T., KOHIYAMA, M., YAMASHITA, T., YAMAMOTO, M., NAKAMURA, N., “Finite-Element Analysis of Laminated Rubber Bearing of Building Frame under Seismic Excitation”, *Earthquake Engineering and Structural Dynamics*, 2015 (in press).

OSGOOEI, P.M, TAIT, M.J., KONSTANTINIDIS, D., ‘‘Three-dimensional Finite Element Analysis of Circular Fiber-reinforced Elastomeric Bearings Under Compression’’, *Composite Structures*, Vol. 108, 2014(a), pp. 191-204.

OSGOOEI, P.M, TAIT, M.J, KONSTANTINIDIS, D., ‘‘Finite Element Analysis of Unbonded Square Fiber-reinforced Elastomeric Isolators (FREIs) Under Lateral Loading in Different Directions’’, *Composite Structures*, Vol. 113, 2014(b), pp. 164-173.

OSGOOEI, P.M, VAN ENGELEN, N.C., KONSTANTINIDIS, D., TAIT, M.J, ‘‘Experimental and Finite Element Study on the Lateral Response of Modified Rectangular Fiber-reinforced Elastomeric Isolators (MR-FREIs)’’, *Engineering Structures*, Vol. 85, 2015, pp. 293-303.

RUSSO, G., PAULETTA, M., “Sliding Instability of Fiber-Reinforced Elastomeric Isolators in Unbonded Applications”, *Engineering Structures*, Vol. 48, 2013, pp. 70–80.

RUSSO, G., PAULETTA, M., CORTESIA, A., “A Study on Experimental Shear Behavior of Fiber-Reinforced Elastomeric Isolators with Various Fiber Layouts, Elastomers and Aging Conditions”, *Engineering Structures*, Vol. 52, 2013, pp. 422–433.

SANCHEZ, J., MASROOR, A., MOSQUEDA, G., RYAN, K., ‘‘Static and Dynamic Stability of Elastomeric Bearings for Seismic Protection of Structures’’, *Journal of structural engineering*, Vol. 139, No. 7, 2012, pp. 1149-1159.

STANTON, J.F, SCROGGINS, G., TAYLOR, A.W., ROEDER, C.W., ‘‘Stability of Laminated Elastomeric Bearings’’, *Journal of Engineering Mechanics*, Vol. 116, No. 6, 1990, pp. 1351-1371.

TOOPCHI-NEZHAD, H., TAIT, M.J., DRAYSDALE, R.G., ‘‘Bonded Versus Unbonded Strip Fiber Reinforced Elastomeric Isolators: Finite Element Analysis’’, *Composite Structures*, Vol. 93, No. 2, 2011, pp. 850-859.

VAN ENGELEN, N.C., OSGOOEI, P.M., TAIT, M.J., KONSTANTINIDIS, D., ‘‘Experimental and Finite Element Study on the Compression Properties of Modified Rectangular Fiber-Reinforced Elastomeric Isolators (MR-FREIs)’’, *Engineering Structures*, Vol. 74, 2014 (a), pp. 52-64.

VAN ENGELEN, N.C., TAIT, M.J., KONSTANTINIDIS, D., “Model of the Shear Behavior of Unbonded Fiber-Reinforced Elastomeric Isolators”, *Journal of Structural Engineering*, 2014(b), *in press* doi: 10.1061/(ASCE)ST.1943-541X.0001120.

VEMURU, V.S.M., NAGARAJAIAH, S., MASROOR, A., MOSQUEDA, G., ‘‘Dynamic Lateral Stability of Elastomeric Seismic Isolation Bearings’’, *Journal of structural engineering*, Vol. 140, No. 8, 2014.

WARN, G.P., WEISMAN, J., ‘‘Parametric Finite Element Investigation of the Critical Load Capacity of Elastomeric Strip Bearings’’, *Engineering Structures*, Vol. 33, No. 12, 2011, pp. 3509-3515.

WEISMAN, J., WARN, G.P., ‘‘Stability of Elastomeric and Lead-Rubber Seismic Isolation Bearings’’, Journal of Structural Engineering, Vol. 138, No. 2, 2012, pp. 215-223.

YAMAMOTO, S., KIKUCHI, M., UEDA, M., AIKEN, I.D., ‘‘A Mechanical Model for Elastomeric Seismic Isolation Bearings Including the Influence of Axial Load’’, *Earthquake Engineering and Structural Dynamics*, Vol. 38, No. 2, 2009, pp. 157-180.